3.5 SCCMS Projects

Developing graph neural networks that helps predicting the molecular dynamics of glassy liquids

Hayato SHIBA
Information Technology Center, University of Tokyo
Kashiwa-no-ha, Kashiwa, Chiba 277-0882

In the past two decades, structure–dynamics correspondence in glass-forming liquids have been hot topic. Along with the drastic slowdown of atomic motion accompanying the glass transition, localized domains of les that rearrange more preferentially than others grow up. Structural analyses of local geometric orders and of real-space normal modes of vibrations have clarified the existence of correlations between the structure and the dynamics. It has remained, however, unclear to what extent the dynamics can be dictated by the structure. Recently, machine learning methodologies, in particular, graph neural networks (GNNs), enabled us to predict the slow dynamics far better than these methodologies. The GNNs have turned out to be a good fit for making predictions more accurately than ever, and thus, open a new paths to further reveal the structure-dynamics relationship.

In FY2022, we have engaged in improving our model, BOTAN (BOnd TArgeting Network), which we have proposed in FY2021. In BOTAN, a decoder for edge features is additionally implemented to the previous GNN model to enable itself to learn relative motion between neighbor pairs (edge target) in addition to self-motion of particles (node target). This model has tens of thousands of weight parameters in it, which is the reason why it can capture the complex relation between the structure and the dynamics. However, in the meawhile, it is difficult to train such a large model, especially when edge features come in as the training target. In order to fix such shortcomings, we have introduced a set of pretrained weight parameters that reflect the fact that closer pairs are more likely to separate in a short-time range. This improvement has updated the best predictive performance even on the time-scale of glassy structural relaxation, see Fig. 1 in which the Pearson correlation coefficients representing the predictive accuracy (τ_α denotes the structural relaxation time). BOTAN is now one of the state-of-the-art models for glassy dynamics relaxation, as well as other models that have also appeared in FY2022. The full article introducing his state-of-the-art model of BOTAN has been published [1], together with training code implemented on PyTorch Geometric [2].

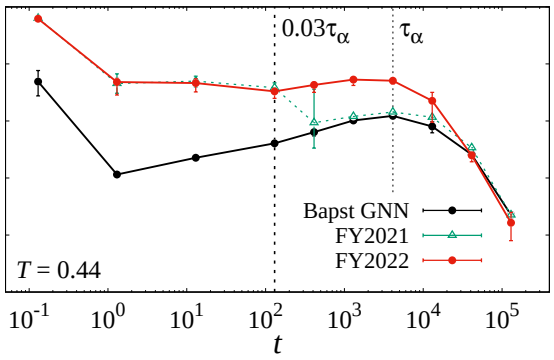

Figure 1: Comparison of pearson correlation coefficients between different GNN models: the original GNN model and of BOTAN (in FY2021 and FY2022).

In FY2022, we have started our next trial to

develop a new application of BOTAN: learning the dynamics of a glassy liquid under quasi-static shear at zero temperature. We have simulated using so-called the Kob-Andersen binary glass-forming mixture and computed the dataset for training by using System B at ISSP, and now we are trying to apply BOTAN for the prediction of rearranging hotspot from the initial structure.

References

[1] H. Shiba, M. Hanai, T. Suzumura, and T. Shimokawabe: J. Chem. Phys. **158**, 084503 (2023).

[2] `https://github.com/h3-Open-BDEC/pyg_botan`

A systematic *ab initio* study of quasi-one-dimensional molecular conductors TM salts

Kazuyoshi Yoshimi[a], Takahiro Misawa[a,b], Takao Tsumuraya[c], and Hitoshi Seo[d,e]
[a] *Institute for Solid State Physics, University of Tokyo, Kashiwa-no-ha, Kashiwa, Chiba 277-8581*
[b] *Beijing Academy of Quantum Information Sciences, Haidian District, Beijing 100193, China*
[c] *POIE, Kumamoto University, 2-39-1 Kurokami, Kumamoto 860-8555, Japan*
[d] *Condensed Matter Theory Laboratory, RIKEN, Wako, Saitama 351-0198, Japan*
[e] *Center for Emergent Matter Science (CEMS), RIKEN, Wako, Saitama 351-0198, Japan*

The quasi-one-dimensional organic conductor TM_2X (TM=TMTSF, TMTTF, X: monovalent anion) has been extensively studied experimentally and theoretically due to its diverse ground states induced by changes in pressure and molecular substitution[1, 2]. While the importance of electronic correlation effects has been pointed out in these studies, a systematic evaluation of electronic correlation effects has not been carried out due to the difficulty of quantitatively estimating electronic interactions in molecular systems.

In this study, we derive effective models using first-principles calculations as a starting point and the constrained random phase approximation method. The analysis of organic conductors involves molecules with many atoms as a unit, which requires significant computational effort and memory to derive effective models. We addressed this problem by using the recently developed software RESPACK[3] and exploiting its parallelization feature to take advantage of large computing resources. Using the first-principles software Quantum ESPRESSO[4] and RESPACK, we systematically derived effective models for TM_2X and analyzed the electronic states using a many-variable variational Monte Carlo solver, mVMC [5].

Based on the obtained results, we discuss the material dependence of the electronic correlation effects in the TM molecular system and clarify the relationship between the different ground states observed in the experiment and the electronic correlation effects. We show that the correlation effect in this system can be characterized by the screened on-site Coulomb interaction U relative to the intrachain transfer integrals. This parameter is material dependent and we show that it plays a key role in understanding the spin and charge ordering phenomena in the system[6].

We thank R. Kato, S. Kitou, and T. Nakamura for fruitful discussions. This work was supported by MEXT/JSPJ KAKENHI under grant numbers 19K03723, 19K21860, 20H04463, 21H01041 and 22K03526. KY and TM were supported by Building of Consortia for the Development of Human Resources in Science and Technology, MEXT, Japan. The input and output files for RESPACK and mVMC are uploaded to ISSP data repository[7].

References

[1] D. Jerome, Chem. Rev. 104, 5565 (2004).

[2] K. Yoshimi, H. Seo, S. Ishibashi, and S. E. Brown, Phys. Rev. Lett. 108, 096402 (2012), and references therein.

[3] K. Nakamura, Y. Yoshimoto, Y. Nomura et al., Comp. Phys. Commun. 261, 100781 (2021).

[4] P. Giannozzi, O. Andreussi, T. Brumme et al., J. Phys.: Condens. Matter 29, 465901 (2017).

[5] T. Misawa, S. Morita, K. Yoshimi et al., Comp. Phys. Commun. 235, 447 (2019).

[6] K. Yoshimi, T. Misawa, T. Tsumuraya, and H. Seo, arXiv:2210.13726.

[7] https://isspns-gitlab.issp.u-tokyo.ac.jp/k-yoshimi/tm-salts

Development of an effective model estimation tool by Bayesian optimization

Kazuyoshi Yoshimi
Institute for Solid State Physics, University of Tokyo
Kashiwa-no-ha, Kashiwa, Chiba 277-8581

Analysis based on effective models is useful to understand properties of materials. The reliability of an effective model is often evaluated by comparing it with experimental data, but this requires trial and error due to the existence of the large number of model parameters. We have developed a tool called Bayesian optimization tool of Effective Models (BEEMs) [1] to estimate effective models as an inverse problem using experimental data and Bayesian optimization with Gaussian processes [2].

In BEEMs, the quantum lattice model solver HΦ[3] is used as the forward solver and the magnetization curves are calculated based on the given Hamiltonian. The cost function is the difference between the obtained magnetization curve and the target magnetization curve. We use the Bayesian optimization library PHYSBO[4] to find the next candidate point of the Hamiltonian that may have a smaller cost function.

BEEMs is available from the GitHub page and can be installed by the following procedures:

```
$ git clone
  https://github.com/k-yoshimi/BEEMs.git
$ cd BEEMs
$ pip3 install .
```

Then, you can use `beems` as a python package. Post tools `gauss_fit`, `mag_plt`, and `output_score` are also available. `gauss_fit` is a tool for constructing a score function using a Gaussian process based on the results obtained by Bayesian optimization. `mag_plot` is a tool for plotting magnetization at specified candidate points. `output_score` is a tool for displaying the score and the candidate point parameters up to the specified rank.

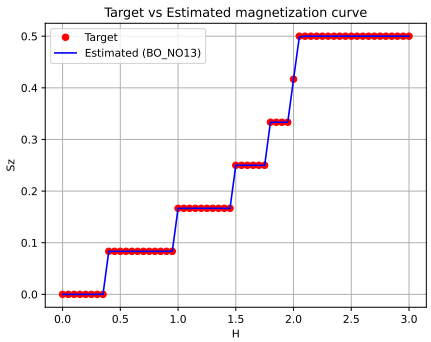

Figure 1: The magnetization curve at $(J_2, J_3) = (0.1, 0.02)$ (represented by red symbols).The proposed magnetization curve using BEEMs (represented by the blue line).

As a demonstration, we performed model parameter fitting for $S = 1/2$ Heisenberg spin chain with 12 sites under periodic boundary condition. The Hamiltonian is given by $\mathcal{H} = \sum_{i=1}^{12} [J_1 \mathbf{S}_i \cdot \mathbf{S}_{i+1} + J_2 \mathbf{S}_i \cdot \mathbf{S}_{i+2} + J_3 \mathbf{S}_i \cdot \mathbf{S}_{i+3}]$. For simplicity, we set $J_1 = 1$ and calculated the magnetization curve at $J_2 = 0.1$ and $J_3 = 0.02$ as the reference data as shown in Fig. 1. Figure 2 shows the mean squared error (MSE) between the reference data and the calculated data. Up to the fifth step, random sampling is performed even if Bayesian optimization is selected. It is seen that after performing Bayesian optimization, the cost function reaches almost zero in the 13th step,

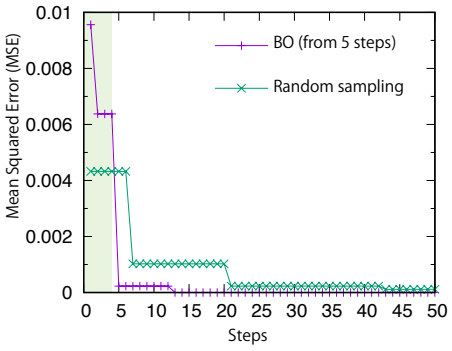

Figure 2: Mean squared error(MSE) between the reference data and the calculated data obtained by the Bayesian optimization (BO) and random sampling, respectively. The green shaded area indicates the region where the random sampling is performed.

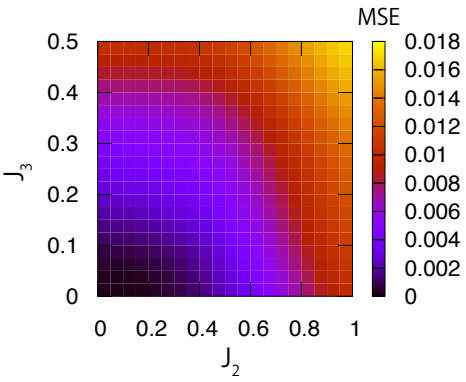

Figure 3: The color map of MSE estimated by the trained model using gaussian process.

while random sampling is underperformed comparing to Bayesian optimization even after 50 steps. The optimal parameters found by Bayesian optimization for the best score are $J_1 = 1.0, J_2 = 0.1$, and $J_3 = 0.025$. We created a trained model using `gauss_fit.py` to estimate MSE obtained with the Gaussian process after 50 trials. As a result, we found that the region where (J_2, J_3) is relatively small has a lower score as shown in Fig. 3. Using such a map, it is possible to check the accuracy of the estimated parameters. For example, we could explore approaches such as refining the grid size in the low score region.

In summary, we have developed BEEMs: an effective model estimation tool by combining HΦ and PHYSBO. In version 1.0, it is possible to estimate the effective model based on the magnetization curve. In the future, we aim to improve the calculation speed, as currently all magnetic fields have to be calculated. We plan to add a mode that can calculate the magnetization curve by splitting the calculation by S_z when S_z is conserved. We also plan to extend the tool to estimate other physical quantities if there is demand. We also plan to provide an expert level manual and allow users to define their own classes for use.

We would like to acknowledge T. Misawa, R. Tamura, and Y. Yamaji for their contribution to code development and useful discussion. KY was supported by JSPS KAKENHI Grant Number 21H01041.

References

[1] https://github.com/k-yoshimi/BEEMs

[2] C.E. Rasmussen and C.K.I. Williams, Gaussian Processes for Machine Learning, The MIT Press (2005).

[3] M. Kawamura, K. Yoshimi, T. Misawa et al., Comp. Phys. Commun. 217, 180 (2017).

[4] Y. Motoyama, R. Tamura, K. Yoshimi et al., Comp. Phys. Commun. 235, 447 (2019).

Exciton Properties in Organic Optoelectronic Devices from Large-Scale Electronic Structure Calculations

Takatoshi Fujita
National Institutes for Quantum Science and Technology
Anagawa, Inage-ku, Chiba 263-8555

Accurate calculations of electronic states are essential for computational studies of organic materials which are directed toward understanding of fundamental processes in organic electronic devices. We have developed the novel large-scale excited-state methods [1] based on the fragment molecular orbital (FMO) method, exicton model, and GW and Bethe-Salpeter equation (BSE) method with Tamm-Dancoff approximation (TDA). In this method, the excited-state Hamiltonian matrix elements at the GW/TDA-BSE level is calculated in the basis of fragment configuration state functions which describe intrafragment excitations or interfragment charge-transfer excitations. The excited-state Hamiltonian is then diagonalized to approximate the adiabatic excited states of an entire system. The novel fragment-based GW/BSE method allows for the efficient calculation of delocalized excited-states in realistic molecular aggregates. In addition, the excited-state Hamiltonian derived this method can be used for real-time simulations in combinations with the wavepacket prorogation method.

We have developed a computational method for excited-state dynamics and time-resolved spectroscopy signals in molecular aggregates [2], on the basis of ab initio excited-state calculations. As an application, we consider the charge separation dynamics and pump–probe spectroscopy in the amorphous P3HT/PCBM blend. To simulate quantum dynamics and time-resolved spectroscopy, the model Hamiltonian for single-excitation and double-excitation manifolds was derived on the basis of fragment-based excited-state calculations within the GW approximation and the BSE. After elucidating the energetics of the electron–hole separation and examining linear absorption spectrum, we investigated the quantum dynamics of exciton and charge carriers in comparison with the pump–probe transient absorption spectra. In particular, we introduced the pump–probe excited-state absorption (ESA) anisotropy as a spectroscopic signature of charge carrier dynamics after exciton dissociation. We found that the charge separation dynamics can be probed by the pump–probe ESA anisotropy dynamics after charge-transfer excitations. The present study provides the fundamental information for understanding the experimental spectroscopy signals, by elucidating the relationship between the excited states, the exciton and charge carrier dynamics, and the time-resolved spectroscopy.

References

[1] T. Fujita, Y. Noguchi, J. Phys. Chem. A **125** (2021) 10580.

[2] T. Fujita, T. Hoshi, https://doi.org/10.26434/chemrxiv-2023-773xs.

Development of an efficient method for calculating miscibility of long-chain polymer blends using molecular dynamics simulations

Kazuo Yamada and Nobuyuki Matubayasi

Division of Chemical Engineering, Graduate School of Engineering Science, Osaka University, Toyonaka, Osaka 560-8531

We have studied the mutual miscibility of polymer species in polymer mixtures using all-atom molecular dynamics simulations. The mutual miscibility of polymers is determined by the free energy of mixing given by the difference between the chemical potentials of the pure and mixed states of the constituent species. Since the chemical potential is sensitive to intra- and intermolecular interactions, an atomistic treatment of polymer mixture systems is desired to evaluate free energy of mixing. However, atomistic calculation of the chemical potential of an entire polymer chain is a difficult task with current computer capabilities because of the enormous number of intramolecular degrees of freedom in polymer chain. To solve this problem, we developed a chain increment method that approaches the chemical potential of polymers using an all-atom model [1]. The intermolecular interaction of a polymer of interest with the surrounding molecules is introduced sequentially for the monomers (segments), and the free energy for turning on the interaction is treated within the framework of a theory of solutions (energy-representation method). In our method, we compute the monomer-wise chemical potential $\Delta\mu_i^{\mathrm{incr}}$ for the incremented monomers in the tagged polymer and the total free-energy of solvation $\Delta\mu$ of the polymer is the sum of $\Delta\mu_i^{\mathrm{incr}}$. This year, we focused on the computation of the free energy of solvation in polymer mixture systems.

Results

The free energy was computed for the mixing of polyethylene (PE) and polyvinylidene difluoride (PVDF) mixture systems with the molar ratio 1:0, 3:1, 1:1, 1:3, and 0:1. The number of the monomer unit n and polymer n_{mol} are fixed 100 and 200, respectively. All-atom molecular dynamics simulation and free-energy calculation has been computed by supercomputer system at ISSP. Figure 1 shows the monomer-wise chemical potential $\Delta\mu_i^{\mathrm{incr}}$ and averaged interaction energy $\langle u\rangle_i$ for each monomer i = 20, …, and 80 by using our scheme [1]. It was seen that both $\Delta\mu_i^{\mathrm{incr}}$ and $\langle u\rangle_i$ are insensitive to the location of the monomer in the inner part of the polymer chain

and depends on the mixing ratio of the polymer systems. The standard error of $\Delta\mu_i^{\mathrm{incr}}$ at i each of i = 20, ... , and 80 is less than ~0.1 kcal/mol for both PE and PVDF at all the molar ratios in Figure 1.

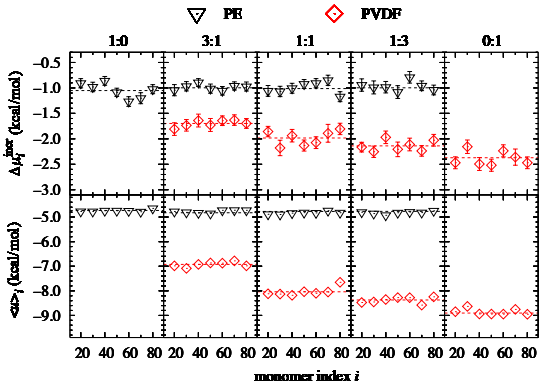

Figure 1: Incremental free energy $\Delta\mu_i^{\mathrm{incr}}$ and the average interaction energy $\langle u\rangle_i$ against the indices i of the incremented PE and PVDF monomers in the PE/PVDF mixture systems.

Figure 2 shows the mixing free energy per monomer $\Delta_{\mathrm{mix}}G/N$ of the PE/PVDF mixture versus the molar fraction of PVDF. According to Figure 1, $\Delta\mu_i^{\mathrm{incr}}$ of PE is within 0.1 kcal/mol over the entire range of mixing ratios, and the mole fraction dependence of $\Delta_{\mathrm{mix}}G/N$ is dominated by that of PVDF. Also, the sign of $\Delta_{\mathrm{mix}}G/N$ is positive for each mixing ratio examined since $\Delta\mu_i^{\mathrm{incr}}$ of PVDF becomes negative for larger mole fractions of PVDF. Figure 2 thus shows that PE and PVDF are immiscible with each other, which is consistent with experimental reports.

Conclusion

When solute degrees of freedom are large, as in polymeric systems, atomistic calculations of solvation free energies are extremely computationally expensive. The chain increment method we have developed approaches free energy of mixing by focusing on the solvation free energy as repeated monomers turn on their interactions with surrounding molecules. Combined with energy-representation method, the pair-wise solvation free energy can be calculated in computational time that is feasible for all-atom MD simulations. Extending this approach to polymer mixtures and applying it to the PE/PVDF system demonstrates that polymer mutual miscibility evaluations can be computed in an all-atom model.

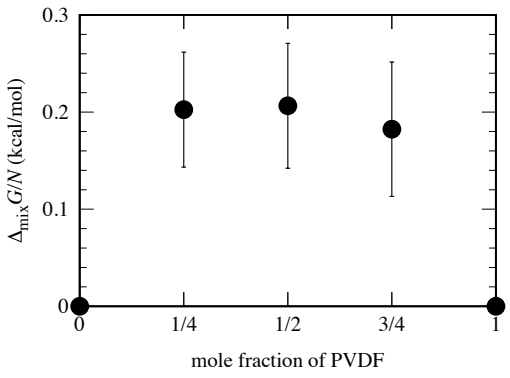

Figure 2: Free energy of mixing per monomer $\Delta_{\mathrm{mix}}G/N$ for the PE/PVDF system at mole fractions of 0, 1/4, 1/2, 3/4, and 1 for PVDF. Since the total number of polymer chains in the system is 200 and the degree of polymerization n is 100 for PE and PVDF, the total number of monomers N is equal to 20000.

References

[1] K. Yamada and N. Matubayasi: Macromol. **53** (2020) 775-788.

Fugaku Battery and Fuel Cell Project

Osamu Sugino

Institute for Solid State Physics,

The University of Tokyo, Kashiwa-no-ha, Kashiwa, Chiba 277-8581

Fiscal 2022 was the final year of the Fugaku-denchi Project [1], in which we participated in the study of the oxygen reduction reaction (ORR) occurring on an oxide electrocatalyst, i.e., zirconium oxynitride. This defective zirconia is known to produce high voltage comparable to platinum under open circuit conditions, but the reaction mechanism is still unknown. Due to the lack of detailed experimental information, we have performed a thought experiment based on reliable first-principles simulations. We first performed a first-principles Monte Carlo simulation with abICS [2] to find a distribution of nitrogen impurities (N_O) and oxygen vacancies (V_O). The results were used to create a model where N_Os and V_Os are located at a subsurface and surface site, respectively. We then investigated the free-energy profile for ORR occurring on the model [3].

Since there are many possible reaction sites for oxide surfaces, we examined all possible adsorption structures of the ORR intermediates and then used a quick and easy method to determine the reaction pathways based on the structural similarity of the intermediates. Among the resulting free energy profiles, we chose those containing relatively small endothermic elementary reactions only. The hydration of OH* was suggested to be the rate determining step under the assumption of minor contribution of the details of activation barrier. The corresponding reaction heat is about 0.4 eV, which is comparable to that on the platinum surface. Importantly, a similar value was obtained for the surface without defects, suggesting that the defects play a minor role in determining the activity of ORR. Experimentally, however, the defects were reported to enhance the reaction current density. A possible explanation for the apparent discrepancy is that defects contribute to increasing the carrier density without changing the activity as much. We are now examining other possibilities as well by using advanced exchange-correlation functionals, increasing the number of possible structures, and considering the activation energies. Making a reliable machine learning potential will be an important step for that purpose.

We are grateful for the opportunity provided by the ISSP supercomputer systems to study the ORR intermediates in detail, which would otherwise be too challenging.

References

[1] https://www.nims.go.jp/fugaku-denchi/en/index.html

[2] https://www.pasums.issp.u-tokyo.ac.jp/abics/

[3] “Effect of Nitrogen Doping and Oxygen Vacancy on the Oxygen Reduction Reaction on the Tetragonal Zirconia (101) Surface”, S. Muhammady, J. Haruyama, S. Kasamatsu, and O. Sugino, J. Phys. Chem. **C126**, 15662–15670 (2022).

Materials design of high performance magnetic materials

Tetsuya FUKUSHIMA
Institute for Solid State Physics, University of Tokyo
Kashiwa-no-ha, Kashiwa, Chiba 277-8581

In this year, we have developed an all electron first-principle calculation code, where a full-potential Korringa-Kohn-Rostoker (KKR) Green's function method is implemented, for the design of permanent magnets and spintronics materials.

It is well known that the local density approximation (LDA) and generalized gradient method (GGA) are poor approaches for strongly correlated materials. In particular, LDA and GGA give unrealistic results for localized f-electron systems. When the electron configurations are not f^7 or f^{14}, the occupied and unoccupied orbitals split off due to the correlation energy. However, in the LDA and GGA calculations, the f orbitals do not split and are pinned on the Fermi energy, leading to significantly overestimated cohesive energy. One of the origin of this problem is the error for self-interaction energy. The Coulomb and exchange terms in a same orbital should be canceled out, because the energy of electron interacts with itself (self-interaction energy) is zero. This is satisfied in Hartree-Fokc approximation; however, LDA and GGA lead to finite self-interaction energy.

We implemented the self-interaction correction (SIC) method to our full-potenital KKR Green' function code and applied it rare earth compounds. In our code, the spherical electron densities of the $4f$ orbitals are extracted from the Green's function, and then the spherical components of the SIC potential are calculated. This means that the our SIC potential is not full-potential. The full-potential SIC is needed to accurately describe the orbital splittings reflecting from the geometric shape of the f orbitals. The SIC potential is constructed by using the exchange correlation potential parameterized by Moruzzi, Janak, and Williams.

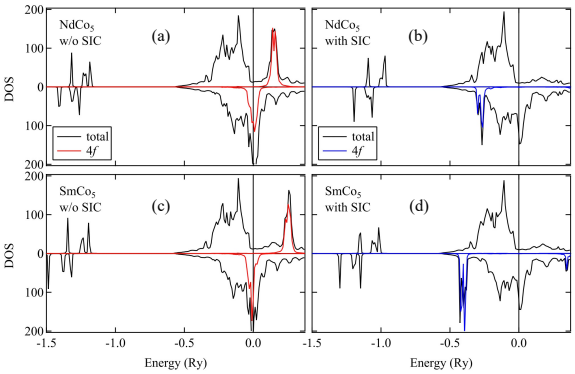

Figure 1: Calculated density of states of $NdCo_5$ and $SmCo_5$. (a,c) and (b,d) correspond to LDA and SIC results, respectively.

In order to investigate the effect of SIC on the electronic structure, we compared the density of states of $NaCo_5$ and $SmCo_5$ calculated by LDA and SIC (see figure 1). We used the experimental lattice constants in these calculations. The space group is $P6/mmm$. As shown in Fig. 1(a,c), in the LDA calculation, the partially occupied f states are located on the Fermi level. On the other hand, SIC lead to the splitting unoccupied and occupied f states. Note that the LDA+U method is often used to correct for such LDA errors, but the value of on-site Coulomb interaction (U) is an empirical parameter and is not suitable for materials screening and design.

Figure 2 shows the density of states of Ce_2O_3

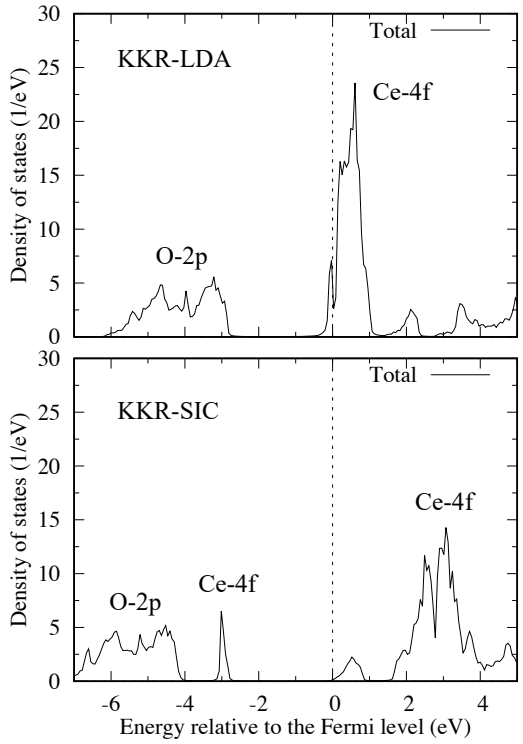

Figure 2: Density of states of Ce_2O_3 calculated by LDA and SIC.

calculated by LDA and SIC. The space group is $\bar{P}3m1$ and the antiferromagnetic state is assumed in the calculations. It is thought that the valence of the Ce ion in Ce_2O_3 is 3+ and the electron configuration f^1 is realized. In the SIC calculation, the occupied f states containing one electron are pushed down to energetically lower region, and are located around -3.0 eV. The unoccupied f states lie around 1.0 eV to 3.0 eV. Pourovskii et al. performed the electronic structure calculations for Ce_2O_3 on the basis of Linear Muffin-Tin Orbital Method with dynamical mean field approximation (DMFT) [1]. Our results obtained from the SIC calculations are quite consistent with their DMFT calculations.

References

[1] L. V. Pourovskii, B. Amadon, S. Biermann, and A. Georges, Phys. Rev. B **76**, 235101 (2007)

Development of high-performance permanent magnets by large-scale simulation and data-driven approach

Takashi MIYAKE
CD-FMat, National Institute of Advanced Industrial Science and Technology
Umezono, Tsukuba, Ibaraki 305-8568

RFe$_{12}$-type compounds with the ThMn$_{12}$ structure are potential main phase for rare-earth magnets. Because of high Fe content, high magnetization and high Curie temperature can be expected. However, RFe$_{12}$ is known to be unstable, and there have been many trials for stabilizing the ThMn$_{12}$ structure by chemical doping. In this study, we investigate the stability of (R,Zr)(Fe,Co,Ti)$_{12}$ (R=Y, Nd, Sm) against the 2-17 and unary phases by first-principles calculation [1].

The calculation is based on density functional theory in the local density approximation. We use AkaiKKR which is based on the Korringa-Kohn-Rostoker Green function method. The open-core approximation is used for the f electrons in Nd and Sm. Randomness caused by doping is treated by coherent potential approximation.

In order to investigate the stability, we consider $R_{1-\zeta_1-\zeta_2-\zeta_3-\zeta_4}\mathrm{Zr}_{\zeta_1}\mathrm{Fe}_{\zeta_2}\mathrm{Co}_{\zeta_3}\mathrm{Ti}_{\zeta_4}$. In the four-dimensional space $(\zeta_1, \zeta_2, \zeta_3, \zeta_4)$, we compare the total energy for the 1-12, 2-17, and unary phases, and identified stable phases. Figure 1 shows the phase diagram of the Sm system on the (Sm,Zr)(Fe,Co)$_{12}$ plane. We then compare the total energy difference between $(R_{1-\alpha}\mathrm{Zr}_\alpha)(\mathrm{Fe}_{1-\beta}\ \mathrm{Co}_\beta\ )_{12-\gamma}$ Ti_γ and stable phases, and calculate the hull distance. Figure 2 shows the result for $(\mathrm{Sm}_{1-\alpha}\mathrm{Zr}_\alpha)(\mathrm{Fe}_{1-\beta}\mathrm{Co}_\beta)_{12}$. We see that the hull distance is not monotonic as a function of α and β. We also see that the hull distance is small for high Zr concentration.

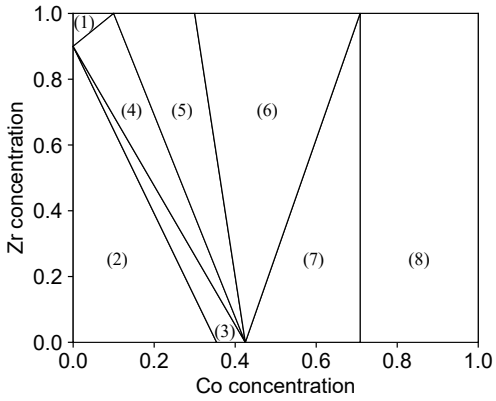

Figure 1: Phase diagram on the (Sm,Zr)(Fe,Co)$_{12}$ plane. (1) (S,Zr)Fe$_{12}$, Zr(Fe,Co)$_{12}$, Zr$_2$Fe$_{17}$ and unary Fe; (2) (Sm,Zr)Fe$_{12}$, Sm$_2$(Fe,Co)$_{17}$, and unary Sm and Fe; (3) (Sm,Zr)Fe$_{12}$, Sm$_2$(Fe,Co)$_{17}$, and unary Fe; (4) (Sm,Zr)Fe$_{12}$, Zr(Fe,Co)$_{12}$, Sm$_2$(Fe,Co)$_{17}$, and unary Fe; (5) Zr(Fe,Co)$_{12}$, Sm$_2$(Fe,Co)$_{17}$, and unary Fe; (6) Zr(Fe,Co)$_{12}$, Sm$_2$(Fe,Co)$_{17}$, Zr$_2$Co$_{17}$, and unary Fe; (7) Sm$_2$(Fe,Co)$_{17}$, Zr$_2$Co$_{17}$, and unary Fe; (8) Sm$_2$Co$_{17}$, Zr$_2$Co$_{17}$, and unary Fe and Co.

References

[1] Taro Fukazawa, Yosuke Harashima, Hisazumi Akai and Takashi Miyake: Phys. Rev. Mater. **6**, 054404 (2022).

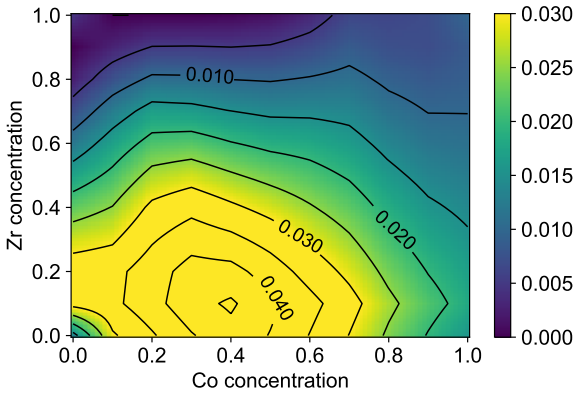

Figure 2: Hull distance in eV for $(Sm_{1-\alpha}Zr_{\alpha})(Fe_{1-\beta}Co_{\beta})_{12}$ with the $ThMn_{12}$ structure.

Data driven analysis for impurity effects on photocatalysts

Mikiya FUJII and Yosuke HARASHIMA
Division of Materials Science, Nara Institute of Science and Technology
Takayama-cho, Ikoma, Nara 630-0192

Photocatalytic generation of hydrogen from solar energy (green hydrogen) is one of the key elements for solving resource, energy, and environmental problems. The purpose of this study is to obtain guidelines for controlling the properties of new photocatalytic compounds and impurities to improve the yield of hydrogen production in response to visible light, which is still not sufficient. For this purpose, a combined analysis of first-principles calculations and informatics will be performed. While materials development has been conducted within a limited search space based on experience, this study will develop a new research in photocatalytic materials development by utilizing information science to predict and develop new materials with a greatly expanded search space. [1, 2] In addition to solving energy problems through hydrogen-producing photocatalysts, this research will have a spillover effect on the synthesis of carbon-neutral petrochemical feedstocks from CO_2 and green hydrogen.

Process informatics for calcination process with dynamical Monte Carlo simulations:

The hydrogen evolution rate (HER) of photocatalytic materials depends strongly on their calcination processes. The calcination process will determine an amount of product compound, defect, and surface area. The HER is considered to be highly dependent on those features, however, experimental analysis to detect the features is time-consuming. We developed a dynamical Monte Carlo (DMC) simulation code to predict the features, and constructed an HER prediction model using the calculated features. The DMC code is written in C++ and the HER prediction code is in Python. The DMC code is based on formation energies of product compounds, defect energies, and surface energies. We will use the first-principles calculation code, Vienna Ab initio Simulation Package (VASP), to calculate these quantities. In Ref. [3], quantum chemical calculations were used as explanatory variables in the model to predict experimental values in flow copolymerization [4]. It was found that information on the so-called transition states of intermediates is important in predicting the products of chemical reactions. This is a kind of data assimilation [5], which we will incorporate into our future method of calculating intermediates in crystal formation by process simulation.

Highthroughput search of high entropy catalyst:

Platinum is known for its high catalytic performance, but it is very rare, so there is a need to develop alternatives. We performed a systematic search for high-entropy alloys that would mimic platinum. The electronic structures were calculated by using first-principles code, AkaiKKR, which is based on the KKR-Green's function method. It enables us to consider nonstoichiometric chemical compositions by the coherent potential approximation. We considered up to a quaternary system which consist of transition metal elements and performed first-principles calculations on more

than 100,000 samples.

References

[1] M. Fujii: JSAP Review, **2022**, 220416 (2022).

[2] 藤井幹也: 応用物理, **91**, 688 (2022).

[3] S. Takasuka, *et al.*: Digital Discovery, accepted.

[4] A. Wakiuchi, *et al.*: Macromol. Mater. Eng. 2200626 (2022).

[5] Y. Harashima: (invited talk) The 24th Annual Meeting of Japan Society of Theoretical Chemistry, May 18th 2023.

Computational and Data Materials Science Study for ET Revolution by Developing Next-Generation Battery and Fuel Cell

Yoshitaka TATEYAMA

National Institute for Materials Science,

Namiki 1-1, Tsukuba, Ibaraki 305-0044

We clarified a long-standing problem of atomistic insight of the dopant effect on the ionic conduction around grain boundary, by extensive first-principles MD calculations of diffusion coefficients[1].

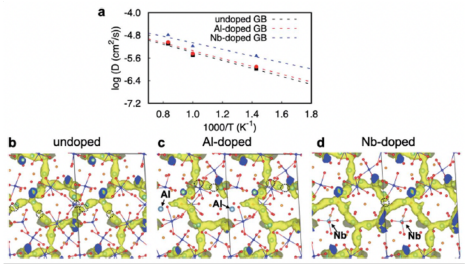

Fig. 1: Calculated self-diffusion coefficients of $Li_7La_3Zr_2O_{12}$ solid electrolyte.

We also developed a high-throughput first-principles MD sampling flow for the ionic conductivity calculations, and proposed potential solid electrolytes with higher ionic conducitivy by applying the flow to Na-ion sulfide solid electrolytes[2].

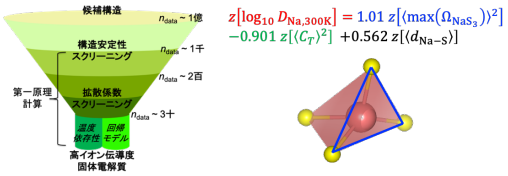

Fig. 2: Schematic picture of the high-throughput screening flow for the search for solid electrolyte materials with the higher ionic conductivities.

We further addressed the speed-up of the conductivity calculations by developing a new method of chemical charge diffusion non-equilibrium MD (CCD-NEMD), and demonstrated that this new method surely accelerates the sampling of mean-square-displacement[3].

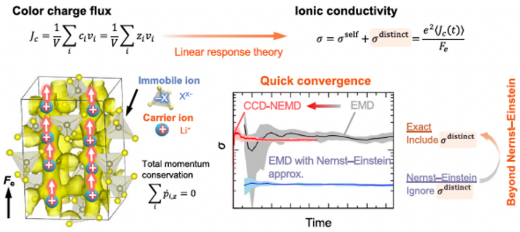

Fig. 3: (left) Definition of flux and color charges to the Li ions and anion units in the $Li_{10}GeP_2S_{12}$ model system. (right) Schematic picture about the speed-up of the evaluation of correlated ionic conductivity.

References

[1] B. Gao, R. Jalem, and Y. Tateyama, J. Mater. Chem. A, **10**, 10083-10091 (2022).

[2] S.-H. Jang, Y. Tateyama, and R. Jalem, Adv. Funct. Mater. **32**, 2206036 (2022).

[3] R. Sasaki, B. Gao, T. Hitosugi, and Y. Tateyama, npj Comput. Mater. **9**, 48 (2023).

Theoretical study of hydrogen-evolution semiconductor photocatalysts using first-principles calculations

Seiichiro L. TEN-NO
Graduate School of System Informatics, Kobe University
Rokkodai-Cho, Nada-Ku, Kobe 657-8501

Planar Defect in Layered Perovskite Photocatalyst $Y_2Ti_2O_5S_2$

Layered perovskite $Y_2Ti_2O_5S_2$ (YTOS) is a promising semiconductor photocatalyst with an electronic structure suitable for overall water splitting under visible light. Similar to other photocatalysts, structural defects during synthesis should be controlled to promote photocatalytic performance [1, 2]. Very recently, transmission electron microscopy (TEM) have revealed extremely large planar defects composed of S–Mg–S layers in YTOS synthesized using the flux method. It is not clear how such a characteristic planar defect makes an effect on photocatalytic activities in YTOS.

Motivated by this observation, we investigated the planar defect structure and electronic structure using first-principles calculations based on the density functional theory (DFT) [3]. The DFT calculations were performed within the PBE+U (Perdew–Burke–Ernzerhof functional with Hubbard U correction) exchange-correlation functional using the projector augmented wave (PAW) method, as implemented in the Vienna ab initio simulation package (VASP). Here we set $U = 7.5$ eV for the $3d$ orbitals at the Ti sites to reproduce the experimental band gap, 1.9–2.0 eV [1].

We have microscopically determined the planar defect structure using the structural optimization, where a Mg atom is centered in the ab-square intersecting the defect S layers (Fig. 1). The obtained defect structure is consistent with the ADF–STEM image: for example, the distance between the Y layers of the defect model, 9.93 Å, is in quantitative agreement with the experimental value, ca. 10.00 Å.

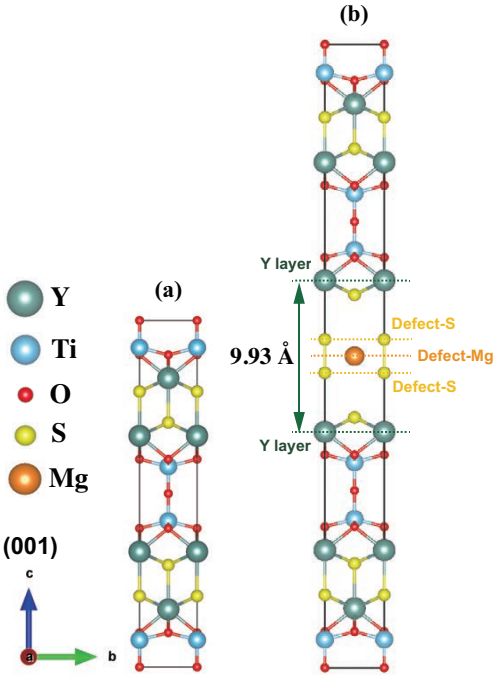

Figure 1: The optimized structure of (a) the conventional unit cell and (b) supercell with the MgS_2 planar defect.

To understand the electronic structures, we have investigated the projected density of states (PDOS) and band structure shown in Fig. 2. The electronic structure shows that the

defect bands appear within the original band gap. The large dispersion of the bands reflects the planar (two-dimensional) nature of the defect in S and Mg with a high state density, in contrast to point defects. It is expected that such defect bands considerably increase the electron–hole recombination rate, enhancing the interband transitions of the defect valence and/or defect conduction bands via radiative or nonradiative transitions, which is an undesirable factor for the efficiency of the overall water splitting of YTOS.

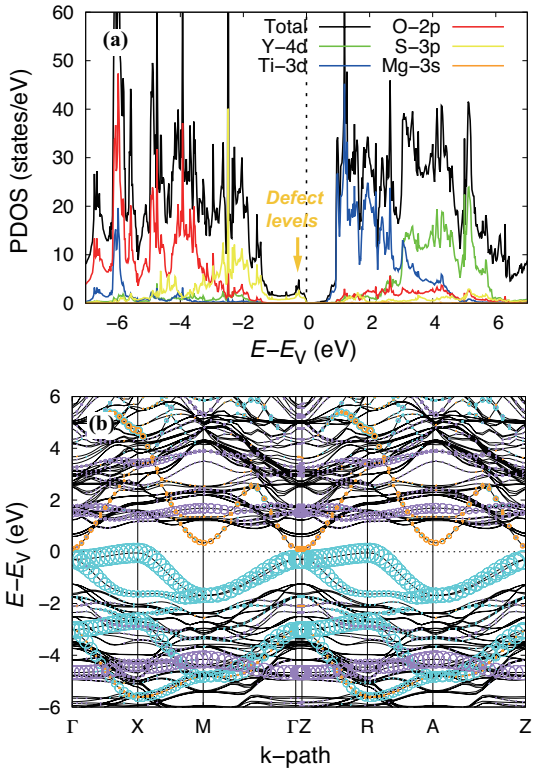

Figure 2: (a) PDOS for YTOS with the planar defect. (b) Band structure with the planar defect. The defect S-3$p_{x,y}$, S-3p_z, and Mg-3s weights are colored in cyan, purple, and orange, respectively. The energy (E) for each case is measured from the valence band maximum (E_{V}).

To consider the stability of the planar defect, we have finally evaluated the defect formation energy (E_{f}). The chemical potentials μ_i were determined by the phase diagram of the relevant compounds in the synthesis of YTOS. Fig. 3 shows E_{f} as a function of the chemical potential of S relative to bulk precipitate ($\Delta\mu_{\mathrm{S}}$), where A, B, and C denote the representive points of the phase diagram. The evaluation of the formation energy suggests that E_{f} increases with decreasing $\Delta\mu_{\mathrm{S}}$ and/or $\Delta\mu_{\mathrm{Mg}}$. Therefore, the optimum conditions for the S and Mg environments must be optimized for the synthesis of YTOS,which suppresses the formation of the planar defect.

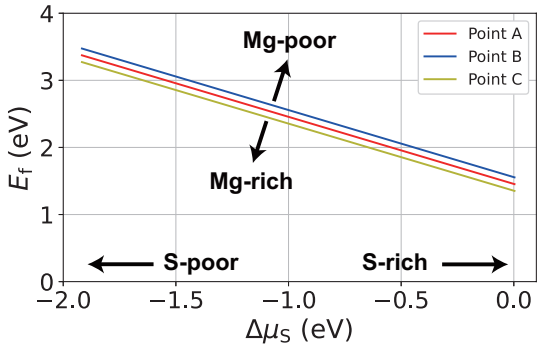

Figure 3: Formation energy of the MgS_2 planar defect E_{f} against $\Delta\mu_{\mathrm{S}}$. The red, blue, and yellow lines represent E_{f} at points A, B, and C of the phase diagram, respectively.

References

[1] Q. Wang *et. al.*: Nat. Mater. **18**, 827 (2019).

[2] Z. Pan *et. al.*: Res. Chem. Intermed. **47**, 225 (2021).

[3] M. Nakabayashi, K. Nishiguchi, X. Liang, T. Hisatomi, T. Takata, T. Tsuchimochi, N. Shibata, K. Domen, and S. L. Ten-no: J. Phys. Chem. C (in press: https://doi.org/10.1021/acs.jpcc.3c00820).